

Article

Soluble Endoglin Stimulates Inflammatory and Angiogenic Responses in Microglia That Are Associated with Endothelial Dysfunction

Eun S. Park ^{1*}, Sehee Kim¹, Derek. C. Yao¹, Jude P.J. Savarraj¹, H. Alex Choi¹, Peng R. Chen¹, and Eunhee Kim^{1,*}

¹ Department of Neurosurgery, McGovern Medical School, University of Texas Health Science Center at Houston; Eunsu.park@uth.tmc.edu (E.S.P.); SeheeKim@uth.tmc.edu (S.K.); Derek.C.Yao@uth.tmc.edu (D.C.Y.); Jude.P.Savarraj@uth.tmc.edu (J.P.S.); Huimahn.A.Choi@uth.tmc.edu (H.A.C.); Peng.R.Chen@uth.tmc.edu (P.R.C.); Eunhee.kim@uth.tmc.edu (E.K.)

* Correspondence: Eunsu.park@uth.tmc.edu (E.S.P.); Tel.: +1-713-500-6129; Eunhee.kim@uth.tmc.edu (E.K.); Tel.: +1-713-500-6837

Abstract: Increased soluble endoglin (sENG) were observed in human brain arteriovenous malformations (bAVMs), and overexpression of sENG with vascular endothelial growth factor (VEGF)-A induced dysplastic vessel formation in mouse brain. However, the underlying mechanism of sENG-induced vascular malformations is not clear. While evidence suggests the role of sENG as a pro-inflammatory modulator, increased microglial accumulation and inflammations were observed in bAVMs. Therefore, we hypothesized that microglia mediate sENG-induced inflammation and endothelial cell (EC) dysfunction in bAVMs. In this study, we confirmed that sENG with VEGF-A overexpression induced dysplastic vessel formation. Remarkably, there were increased microglial activation around dysplastic vessels with expression of NLRP3, inflammasome marker. We found that sENG increased the gene expression of VEGF-A, pro-inflammatory cytokines/inflammasome mediators (TNF- α , IL-6, NLRP3, ASC, Caspase-1, and IL-1 β), and proteolytic enzyme (MMP-9) in BV2 microglia. The conditioned media from sENG-treated BV2 (BV2-sENG-CM) significantly increased angiogenic factors (Notch-1 and TGF β) and pERK1/2 in ECs while it decreased IL-17RD, an anti-angiogenic mediator. Finally, the BV2-sENG-CM significantly increased EC migration and tube formation. Together, our study demonstrates that sENG provokes microglia to release angiogenic/inflammatory responses which may be involved in EC dysfunction. Our study suggests the contribution of microglia in the pathology of sENG-associated vascular malformations.

Keywords: brain arteriovenous malformation (bAVM); soluble endoglin (sENG); microglia; endothelial cells (ECs); inflammation; angiogenesis

1. Introduction

Brain arteriovenous malformations (bAVMs) are an abnormal tangle of enlarged vasculature in brain caused by a direct connection of arteries and veins without an intervening capillary bed [1, 2]. Although bAVMs are rare (about one in 2,000–5,000 people), it is the major cause of intracerebral hemorrhages in children and young adults as well as other neurological symptoms such as seizures, headache, and difficulty in movement, speech, and vision [1, 3–5]. Currently, the pathophysiology of bAVMs are poorly understood and the treatment options for bAVM are limited mostly relying on surgical resection, endovascular embolization or radiation.

Endoglin (ENG) is a type I transmembrane glycoprotein which is mainly expressed in vascular endothelial cells (ECs) and activated monocytes [6]. ENG modulates transforming growth factor- β (TGF β) superfamily signaling and regulates endothelial quiescence and angiogenesis, and its mutation results in hereditary hemorrhagic telangiectasia

type 1 (HHT1), an autosomal dominant vascular disorder [7, 8]. Previous studies have shown that soluble ENG (sENG), circulating cleaved form of ENG, was related to development of sporadic bAVMs [9]. For instance, plasma sENG levels were elevated in human bAVM patients [9]. A focal overexpression of sENG with overexpression of vascular endothelial growth factor (VEGF)-A induced vessel dysplasia in mice [9]. However, exact mechanism of sENG-induced abnormal vascular formation remains to be clarified.

Increased inflammation is observed in bAVMs [10-13]. Enhanced accumulation of microglia was observed around bAVMs in human patients and mouse models of bAVM [12, 13]. Inflammatory cytokines were increased in bAVM tissues as well as the patient's blood [12, 13]. While this evidence suggests that inflammation is critical in bAVM pathophysiology, pro-inflammatory activity of sENG has been shown. Soluble ENG enhanced oxidative stress and activation of matrix metalloproteinases (MMP-2 and MMP-9), the mediators of inflammatory response, in sENG/VEGF-A-overexpressing mouse brain [9]. Studies have also shown that sENG increased nuclear factor-kappa B (NFkB) activation and interleukin-6 (IL-6) expression in cultured ECs [14].

Based on the roles of sENG and microglia in inflammation and bAVMs, we hypothesized that sENG-stimulated microglia is involved in vascular abnormality by inflammatory and angiogenic responses. In this study, we found that systemic sENG administration induced dysplastic capillaries over the VEGF overexpression. We also observed increased activated microglia expressing NLRP3, an inflammasome marker, around the abnormal vessels. *In vitro* studies further revealed that sENG-stimulated BV2 microglia expressed inflammatory and angiogenic factors, and the conditioned medium from sENG-treated BV2 significantly increased angiogenic markers and migration/tube formation in ECs. These results suggest that microglia may contribute to sENG-induced endothelial dysfunction via releasing inflammatory and angiogenic factors. The microglia-mediated endothelial dysfunction can be a possible mechanism underlying sENG-induced bAVMs.

2. Results

2.1. Soluble ENG induced vascular dysplasia in mouse brain with VEGF overexpression

Previous study showed that focal brain overexpression of VEGF-A and sENG resulted in the formation of dysplastic vessels [9]. Since enhanced circulating sENG has been detected in bAVM patients, we systemically injected recombinant human sENG in the mice with focal brain VEGF-A overexpression by intracerebral injection of AAV1-VEGF-A (Fig. 1A). Blue latex casted brains clearly showed dysplastic and enlarged vasculatures in mice with sENG treatment and VEGF-A overexpression. The dysplastic vessels formed around AAV-VEGF-A-injected site (ipsilateral) (Fig. 1B), and the volume of dysplastic vessels were significantly increased compared to normal vessels in the other hemisphere without AAV-VEGF-A injection (contralateral) (Fig. 1B,C). Dysplastic vessels were not found in mouse brain with VEGF overexpression alone without sENG injection or sENG treatment with control AAV1-LacZ injection (Fig. 1C). By immunostaining using CD31 antibody, we confirmed significantly enlarged vessels in the brains of mice with VEGF-A overexpression and sENG administration (Fig. 1D). These data suggest that the sENG with VEGF-A overexpression causes vascular malformations.

2.2. Microglia with enhanced inflammasome marker were recruited around sENG/VEGF-A-induced dysplastic vessels in mice

Brain AVM patients and mouse models displayed microglial activation and increased inflammatory markers in bAVM tissues [11, 12, 15, 16]. In this study, we determined the microglial activation around sENG/VEGF-A-induced dysplastic vessels by Iba-1 immunostaining. Iba-1-positive (+) activated microglia were localized around sENG-injected lesions (Fig. 2A) with a significantly higher fluorescence intensity of Iba-1 exhibiting a thick cell body compared to the one in control mice administrated with AAV1-VEGF-A or sENG alone. The microglia in control mice showed a small cell body and long branches [17-19] (Fig. 2B).

Preeclampsia patients who have a high level of sENG and inflammatory cytokines in plasma, have shown NLRP3-mediated inflammasome activation in their placenta [20]. To test if the sENG/VEGF-A activates inflammasome in the microglia around dysplastic vessels, we further performed immunostaining using NLRP3 with Iba-1 and CD31 antibodies. The accumulated microglia around dysplastic vessels showed a remarkable NLRP3+ signals compared to the normal vessels (Fig. 2A). The fluorescence intensity of NLRP3 was significantly increased in the activated microglia around the dysplastic vessels (Fig. 2A,C). The data suggest the potential role of activated microglia with inflammasome activation in sENG/VEGF-A-induced vascular malformation.

2.3. Soluble ENG induced expression of VEGF-A and inflammatory/inflammasome markers in cultured microglia.

To test if sENG stimulates microglia to enhance inflammatory/inflammasome activation, we measured inflammatory/inflammasome markers in cultured BV2 microglia treated with sENG. The results showed that sENG significantly increased mRNA levels of VEGF-A, tumor necrosis factor (TNF)- α , IL-6, and MMP-9 (Fig. 3A) and inflammasome markers, including NLRP3, apoptosis-associated speck-like protein containing a caspase recruitment domain (ASC), caspase-1, and IL-1 β (Fig. 3B). The data demonstrate that sENG induces inflammatory/inflammasome responses in microglia.

2.4. Soluble ENG-stimulated microglia modulated angiogenic factors in endothelial cells.

While uncontrolled excessive angiogenesis is considered as a hall mark of bAVM development [21], it has been shown that microglia-derived angiogenic and inflammatory mediators were associated with enhanced angiogenesis in ECs [22]. To test if sENG-treated microglia regulate angiogenic property of ECs, we measured expression of TGF β , Notch-1, and phospho (p)-ERK1/2, the angiogenic factors that have been related to bAVM development [16, 23-29], in ECs treated with BV2-conditioned media (BV2-sENG-CM). BV2-sENG-CM significantly increased TGF β and Notch-1 gene expression in ECs compared to controls treated with vehicle or sENG only (Fig. 4A). BV2-CM (the CM from BV2 without sENG treatment) significantly increased p-ERK1/2 levels in ECs, and BV2-sENG-CM further enhanced the p-ERK1/2 levels. The direct treatment of sENG to ECs also induced the ERK1/2 activation, however the levels were smaller compared to the levels in ECs treated with BV2-sENG-CM (Fig. 4B). We further determined the expression of IL-17 receptor D (IL-17RD) which is downregulated in a high angiogenic niche such as cancer [30, 31]. BV2-sENG-CM significantly decreased the level of IL-17RD in ECs while direct treatment of sENG did not affect the levels in ECs (Fig. 4C). These results suggest that microglial secreting factors mediate the regulation of sENG-induced angiogenic response in ECs.

2.5. Soluble ENG-stimulated microglia modulated endothelial cell functions.

Altered EC functions such as enhanced proliferation, migration, or tube formation has been associated with pathologic angiogenesis and abnormal vessel formation [32-34]. We, therefore, tested if the sENG-treated BV2 regulate ECs functions. In a scratch-wound assay, BV2-sENG-CM treatment showed faster EC migration compared to sENG- or BV2-CM-treated ECs (Fig. 5A). By tube formation assay using matrigel, we also confirmed that BV2-sENG-CM significantly increased the total tube length and the branch and loop counts in ECs compared to the controls suggesting the enhanced tube formation (Fig. 5B). The data demonstrate that sENG-treated microglia modulate the EC functions.

2.6. Figures

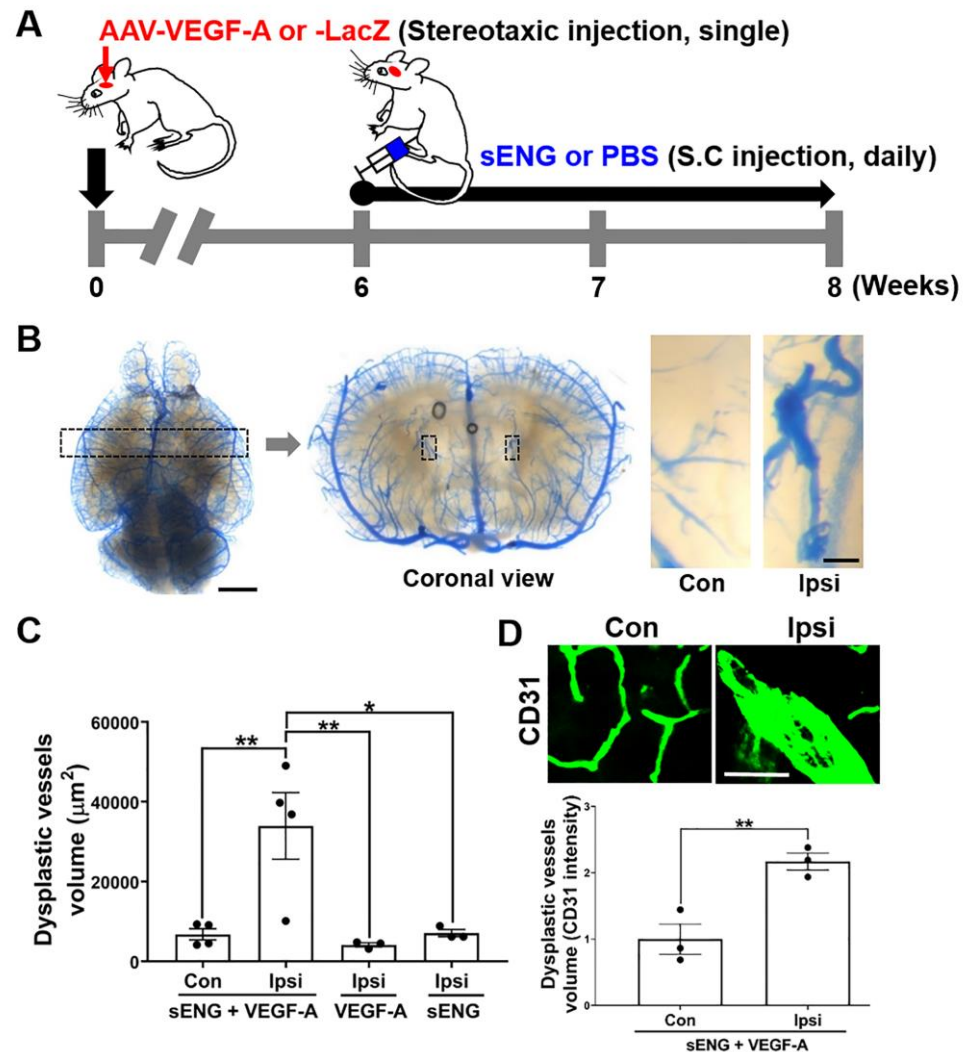


Figure 1. Soluble ENG/VEGF-A induce formation of dysplastic vessels in the mouse brain. (A) Experimental scheme for sENG and VEGF-A injection. The mice were stereotaxically injected AAV-VEGF-A (or AAV-LacZ) into the intra-striatum and administered recombinant sENG (or PBS) subcutaneously (s.c) every day for two weeks from six weeks after the AAV-VEGF-A injection. At 8 weeks after the AAV-VEGF-A injection, the mice were sacrificed. (B) Representative images of latex-casted-brains in mice injected with sENG and AAV-VEGF-A. Coronal sections showed the enlarged abnormal vasculature (inset) in AAV-VEGF-A injected site (ipsilateral) compared to non-injected site (contralateral). Scale bars: 2 mm (whole brain image) and 100 μm (Inset). (C) The quantification of vessel volume in mouse brains. sENG+VEGF-A, mice injected with sENG and AAV-VEGF-A, VEGF-A, mice injected with vehicle (PBS) and AAV-VEGF-A, sENG, mice injected with sENG and AAV-LacZ, $n=3-4$, * $P<0.05$, ** $P<0.01$, One-way ANOVA. (D) Image of CD31 immunostained brain from mice injected with sENG and AAV-VEGF-A and the quantification of CD31 intensity, Scale bar: 50 μm , $n=3$, ** $P<0.01$, Student's t -test. Con, contralateral, Ipsi, ipsilateral.

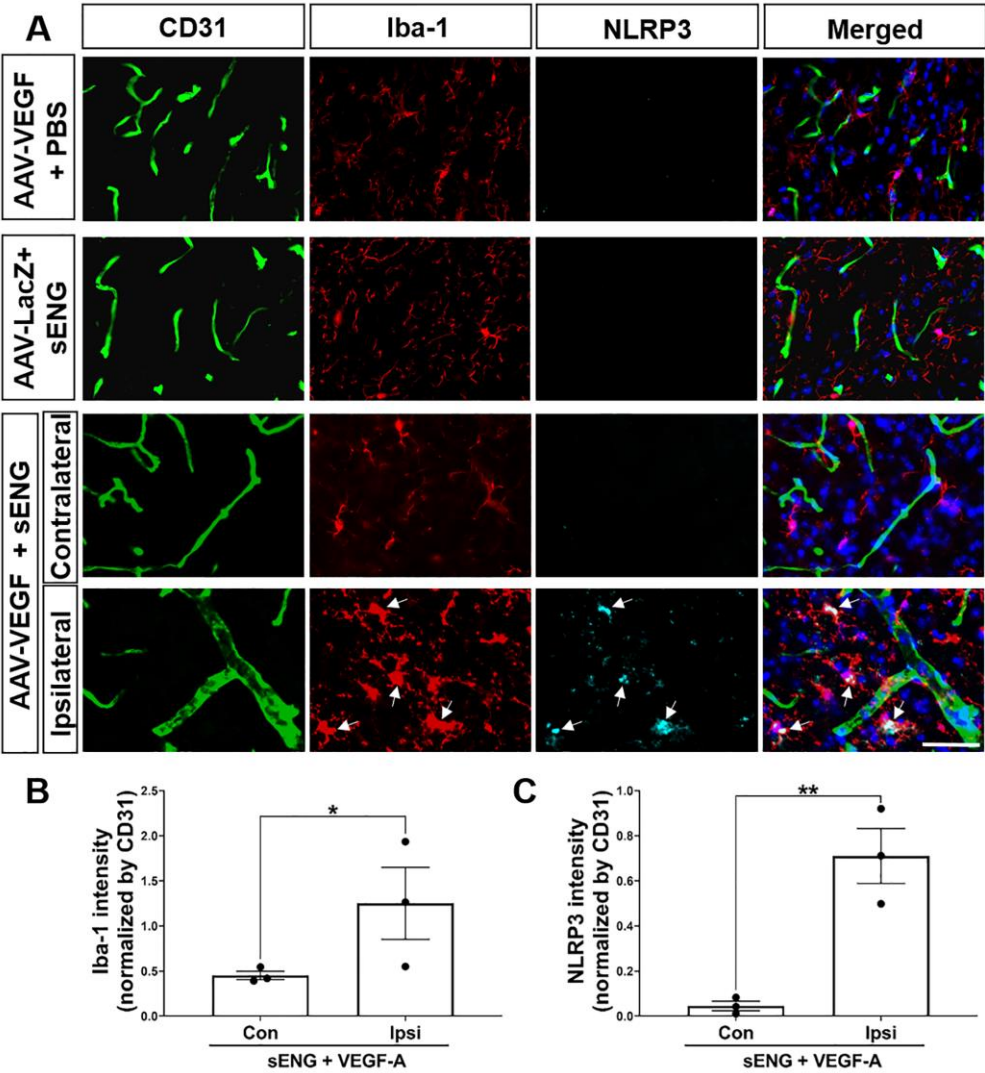


Figure 2. Soluble ENG/VEGF-A induces microglial activation and expression of inflammasome marker around dysplastic capillaries in mouse brain. (A) Immunostaining of mouse brain with CD31, Iba-1, and NLRP3 antibodies. Iba-1+ activated microglia are distributed around sENG/VEGF-induced dysplastic vessels in mouse brain. Iba1+/NLRP3+ cells (arrows) indicate the inflammasome activation within activated microglia. Scale bar: 50 μ m. (B,C) The quantification of intensity of Iba-1 (B) and NLRP3 (C) fluorescence normalized by CD31, respectively. n=3, * P <0.05, ** P <0.01 vs contralateral. Student's t -test.

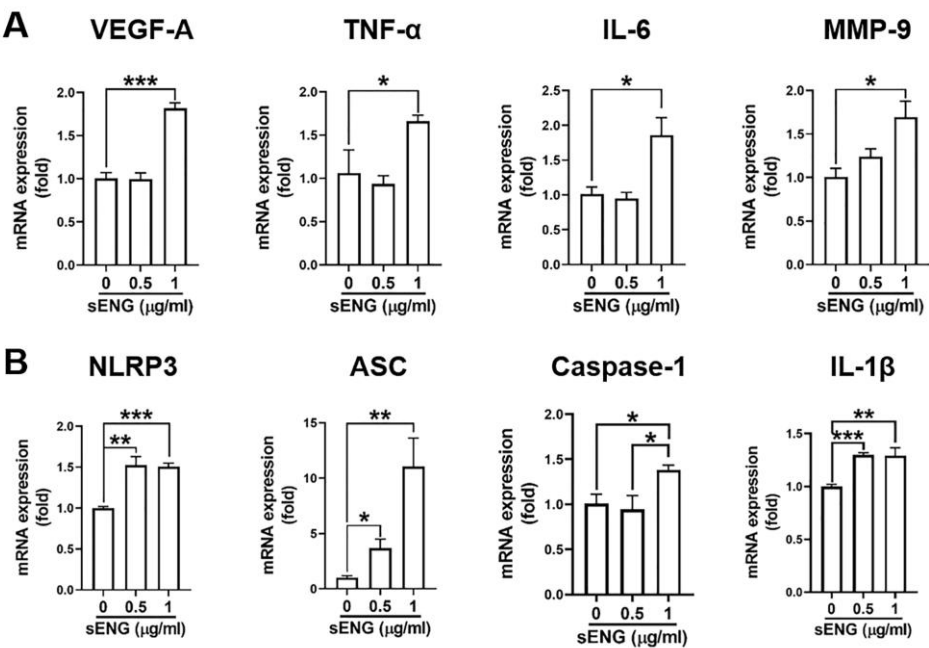


Figure 3. Soluble ENG induced gene expression of angiogenic and inflammatory mediators in microglia. (A,B) Change of gene expression levels of angiogenic mediator and inflammatory cytokines (A) and inflammasome markers (B) in BV2 microglia by sENG treatment. BV2 cells were stimulated with 0.5 or 1 μg/ml of sENG for 24h. The each mRNA levels were normalized with GAPDH. n=3, **P*<0.05, ***P*<0.01, ****P*<0.001. Student's *t*-test.

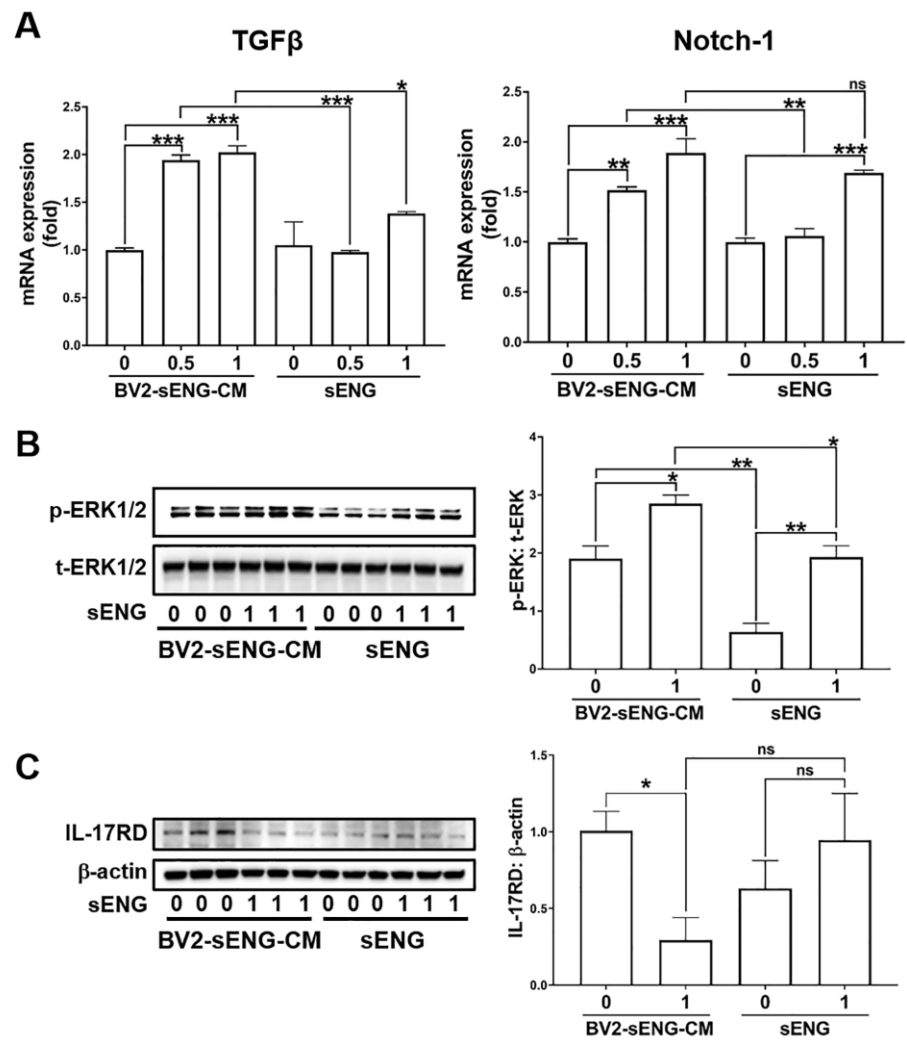


Figure 4. Soluble ENG-stimulated microglia regulate expression of angiogenic mediators in endothelial cells. (A) Gene expression of angiogenic mediators in ECs treated with sENG (0.5 or 1 μg/ml)-treated microglia conditioned medium (BV2-sENG-CM). BV2-CM, BV2-sENG-CM, PBS, or sENG were incubated for 24 hours in mouse brain vascular endothelial cells (ECs) and measured the mRNA levels. * $P<0.05$, ** $P<0.01$, *** $P<0.001$. One-way ANOVA. **(B)** BV2-sENG-CM or sENG induces p-ERK1/2 expression in ECs. $n=3$, * $P<0.05$, ** $P<0.01$ One-way ANOVA. **(C)** BV2-sENG-CM decreases IL-17RD expression in ECs. $n=3$, * $P<0.05$ One-way ANOVA.

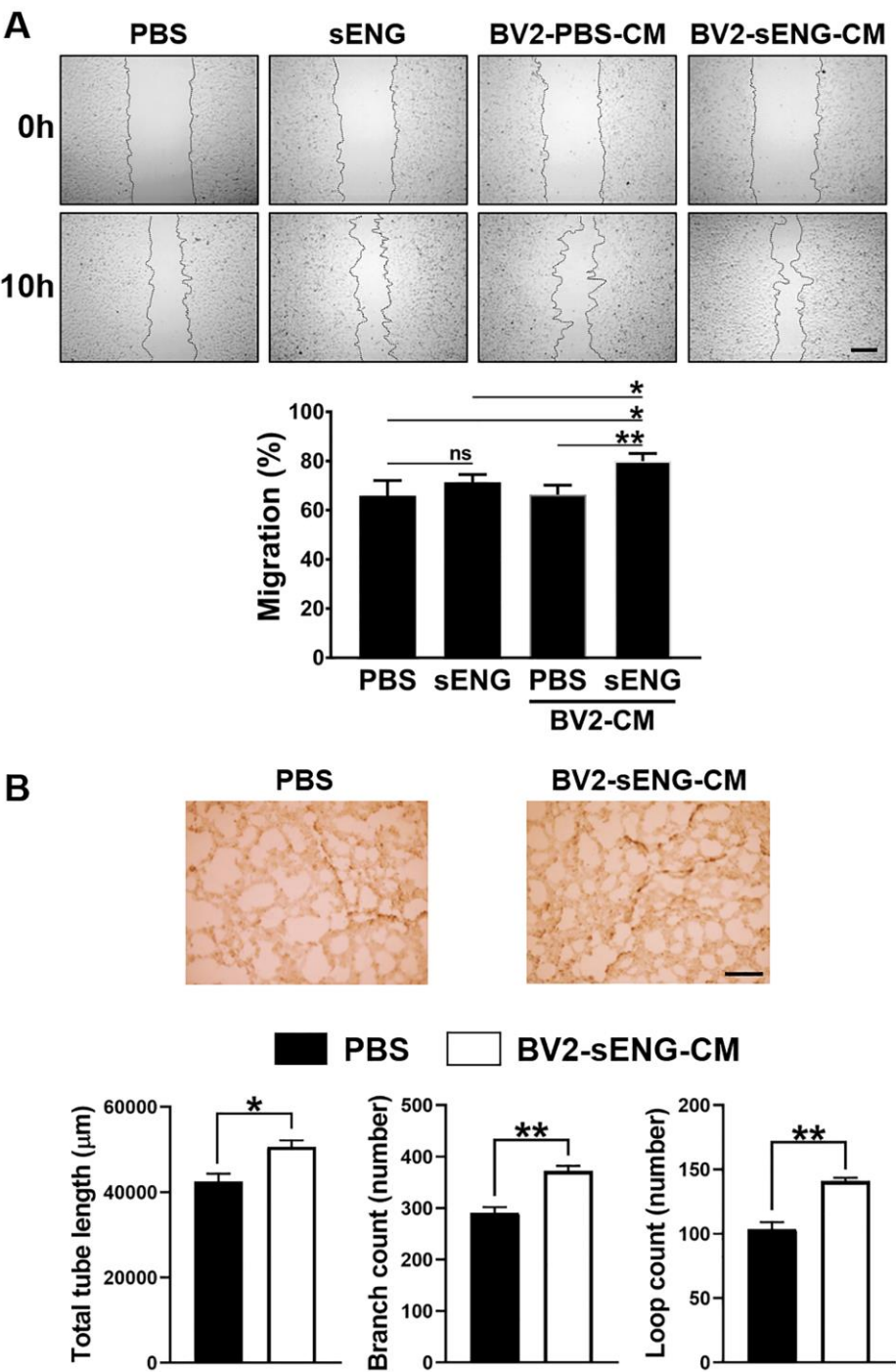


Figure 5. Soluble ENG-stimulated microglia induces hyper-angiogenic phenotype of endothelial cells. (A) BV2-sENG-CM induced EC migration in a scratch-wound assay. The rate of EC migration in each treatment was quantified the distance between the edges of scratched area at 10 h compared to 0 h after the scratch. n=3, * $P<0.05$, ** $P<0.01$. Scale bar: 400 μm. **(B)** BV2-sENG-CM increased endothelial tube formation. The tube length, branch count, and loop count were automatically and blindly measured using Ibidi software. Three independent experiments were performed and representative images are shown. n=3, * $P<0.05$, ** $P<0.01$, Student's *t*-test. Scale bar: 500 μm.

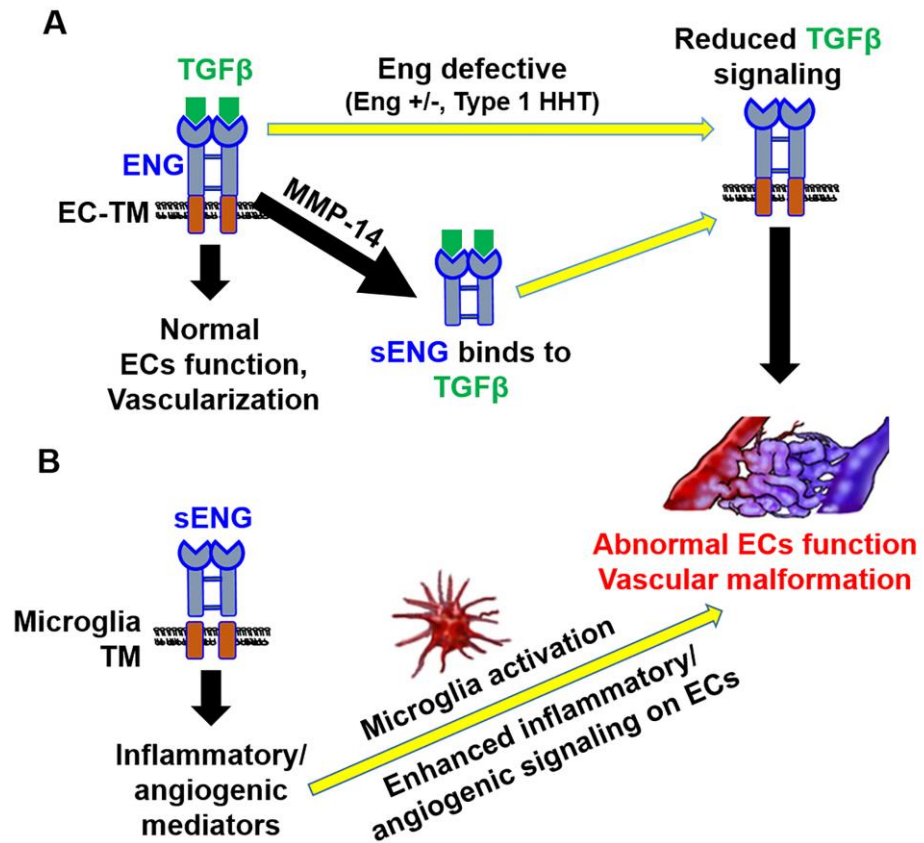


Figure 6. The role of soluble ENG in endothelial dysfunction and vascular malformation. Endoglin (ENG) mediates TGFβ signaling pathway in endothelial cells (ECs). The mutation of Eng (haploinsufficiency) reduces TGFβ signaling. MMP-14 cleaves the extracellular domain of ENG in ECs producing soluble form of ENG (sENG). The sENG acts as a decoy receptor for the TGFβ, and results in impaired TGFβ signaling. Therefore, both mutant ENG and sENG lead to disruption of TGFβ signaling and subsequently mediate ECs dysfunction and vascular malformation. TM, transmembrane. **(B)** Soluble ENG stimulates microglia by unknown mechanism and leads to microglial activation with up-regulation of inflammatory/angiogenic mediators. The microglia-derived inflammatory/angiogenic mediators possibly induce hyper-angiogenic signaling on ECs and ECs dysfunction. Taken together, the sENG-induced disrupted TGFβ signaling in ECs and activation of microglia may synergize to drive vascular malformations.

3. Discussion

In the present study, we demonstrated that microglia were activated around dysplastic/enlarged vessels induced by systemic sENG injection with focal overexpression of VEGF. We also revealed that sENG increased angiogenic and inflammatory/inflammable mediators in microglia, and finally showed that sENG-treated microglia regulated angiogenic property of ECs via the releasing factors. This is the first study that demonstrates the association of microglia in the sENG-induced endothelial dysfunction providing a novel insight in inflammatory response in bAVM pathology.

TGFβ signaling pathway is essential for vessel development and the maintenance [35, 36], and impairment of the signaling is associated with cerebrovascular disease, including AVMs and aneurysms [25]. In particular, the TGFβ receptor, Eng- or Alk1-hap-

loinsufficiency with a focal VEGF-A overexpression disrupts TGF β signaling causing development of HHT type 1 or 2-associated AVMs in mice [37, 38]. Meanwhile, enhanced activity of MMPs (e.g., MMP-14) is observed in bAVMs and involved in the sENG production by ENG cleavage [9, 39-41]. Although the exact mechanism how sENG disrupts the TGF β signaling remains to be clarified, sENG can bind to circulating TGF β or BMP9, the ligands of Alk1 causing the reduced activation of TGF β pathway that would consequently result in abnormal ECs function and vascular malformation (Fig. 6A) [42, 43]. Evidences have shown that sENG:BMP9 or sENG:TGF β complex were detected in plasma of preeclampsia patients [43-45].

Elevated sENG levels have been seen in human bAVM tissues, and focal overexpression of sENG and VEGF-A by virus system induced vascular dysplasia [9]. Based on these findings, our study tested if systemic administration of sENG leads to development of abnormal vascular formation. We confirmed that recombinant sENG consistently induced vascular dysplasia in the focal area injected with AAV-VEGF-A (Fig. 1). Our results showing that VEGF-A overexpression without sENG or sENG administration without VEGF overexpression did not induce the dysplastic vessel development (Fig. 1C) support that both defective ENG function and VEGF-A are required in abnormal vascular development [46].

The mechanism in which sENG/VEGF-A induces vascular dysplasia is unclear. While high levels of sENG have been identified in several other human pathological conditions (preeclampsia, coronary atherosclerosis, Alzheimer's disease, hypertension and diabetes) related to dysregulated vascular permeability, endothelial function, and/or angiogenesis [43, 47-49], our study shows that sENG is involved in microglia-mediated inflammation. Our immunostaining data shows that the microglial activation with enhanced NLRP3, an inflammasome marker, around sENG/VEGF-induced dysplastic vessels (Fig. 2) suggesting the role of microglia in the abnormal vascular development. Supportively, our *in vitro* study confirmed that sENG increased VEGF-A, inflammatory cytokines, and inflammasome markers in BV2 microglial cells (Fig. 3) and BV2-sENG-CM treatment enhanced the expression of angiogenic mediators (Fig. 4) and functions in ECs (Fig. 5). Taken together, these *in vivo* and *in vitro* data suggest that microglia may accelerate abnormal function of ECs and contribute to abnormal vascular development upon increased circulating sENG.

Our findings suggest pro-angiogenic effects of sENG, however previous studies have shown that sENG can inhibit endothelial tubulogenesis and cell migration [50]. A previous study has shown that 100 ng/ml of sENG reduced EC migration in a scratch wound assay [50]. However, our study using 1000 ng/ml of sENG did not reduced EC migration. In addition, BV2-sENG-CM exhibited the faster migration and higher tube formation in ECs (Fig. 5). It remains to be defined if EC functions are differentially regulated depending on sENG concentration, however our results clearly show the role of microglia in mediating the sENG effect in EC functions. With the previous evidence demonstrating the role of microglia in vascular architecture via regulating TGF β signaling in ECs [51], our study suggest that the sENG-induced microglial activation may be sufficient to compensate the sENG-induced loss of TGF β signaling in EC. It is partially supported by the increased TGF β expression in ECs treated with BV2-sENG-CM (Fig. 6B).

Microglia are involved in a broad range of brain functions, including control of neuronal synapse development, normal myelinogenesis or oligodendrocyte progenitor maintenance, phagocytosis of apoptotic cells, and brain repair [52-57]. However, their role in bAVM pathology is not clear yet. The capillary-associated microglia closely interact with ECs, astrocytes, and pericytes composing brain microvascular unit and blood-brain barrier (BBB) [58-60]. In the pathologic condition such as bAVM, the damaged ECs can be the source of sENG [9]. The sENG shredded from damaged ECs may stimulate the microglia, and the factors from activated microglia (including angiogenic/inflammatory mediators) would subsequently lead to ECs dysfunction. The expression of ENG on microglia/macrophage in healthy or pathologic brain such as Alzheimer's disease or Parkinson's disease [61-64]. Therefore, sENG can be also generated from microglia as well as

ECs, and have the possibility of autocrine effects on microglia. However, it is not clear how sENG stimulates microglia. The detailed mechanisms by which sENG activate the microglia should be determined.

Targeting immune cells are emerging approach in cerebrovascular disease, including aneurysm and bAVM [65]. Even though there were obvious inflammatory reactions and immune cell accumulation in human and mouse bAVM [11, 12, 16], the significance of immune cells in bAVM pathophysiology has been overlooked. Our study provides a set of evidence demonstrating that microglia contributes to sENG-induced EC dysfunction and supporting the possible critical role of microglia in bAVM pathology. Further study to define the exact mechanism how microglia regulates the EC dysfunction will ultimately provide novel insights to develop therapeutic strategies for bAVM patients by targeting microglia and the associated inflammation.

4. Materials and Methods

Animals

All experiments performed in accordance with the approved animal protocols by Center for Laboratory Animal Medicine and Care (CLAMC) in the University of Texas Health Science Center at Houston. Male C57BL/6 mice (8 weeks of age, 23–25 g) were housed under a 12:12 h light:dark cycle at an ambient temperature of 22°C. Water and mouse chow were available ad libitum. Young male mice were selected in this study because the bAVM usually diagnoses in young males [66, 67].

Treatment of AAV-VEGF-A and sENG in mice

Adeno-associated viral (AAV) mediated vascular endothelial growth factor (AAV1-CMV-hVEGF-A, 2 μ l, 2×10^9 gc/ml, Vector Biolabs, Malvern, PA) or AAV1-LacZ (2 μ l, 2×10^9 gc/ml, Vector Biolabs) was stereotactically injected into the right striatum (anteroposterior: 0.5 mm, mediolateral: 2.0 mm, and dorsoventral: 3.0 mm from bregma) according to the mouse brain atlas. At six week after the AAV1-VEGF-A injection, recombinant human sENG protein (4 μ g/kg, 1097-EN-025, R&D systems, Minneapolis, MN) was daily injected subcutaneously for 14 days. PBS was injected as control.

Systemic latex vascular casting and analysis

To visualize the brain vasculature, systemic latex dye perfusion was performed. Blue latex dye (BR80B, Connecticut Valley Biological, Southampton, MA) were injected into the left ventricle of the heart. Brain was collected and fixed in 10% neutral buffered formalin solution (HT501320, Sigma-Aldrich, St. Louis, MO). Brain was sequentially dehydrated with a series of methanol (A412-4, Fisher Scientific, Hampton, NH), (50, 75, 95 and 100 % in each 24 hr), and cleared in benzyl benzoate (AC105862500, ACROS organic, New Jersey) and benzyl alcohol (AC148390010, ACROS organic), (1:1 ratio). The each single dysplastic lesion images were captured under a 30x magnification using a light microscope (Zeiss SteREO Discovery. V12). To measure the dysplastic vessel size, the region of interests (ROI's) were drawn with a spline contour and automatically quantified by Zen 2.3 software by a blinded expert.

Immunofluorescence staining and analysis

Animals were transcardially perfused with PBS and fixed with 10% formalin. Collected brain were sectioned (30- μ m thick) for immunohistochemical staining. Sections were incubated overnight with the following primary antibodies: mouse anti-CD31 (1:1,000, AF3628, R&D systems) for endothelial cells (ECs), rabbit anti-Iba-1 (1:1,000, 019-19741, Wako, Richmond, VA) for microglia, goat anti-NLRP3 (1:200, MAB7578, R&D systems) for inflammasome marker. After the incubation with primary antibodies, tissues were incubated with 488-conjugated donkey anti-goat IgG (1:500, 705-545-147, Jackson ImmunoResearch, West Grove, PA) for CD31, 647-conjugated donkey anti-rabbit IgG

(1:500, 711-605-152, Jackson ImmunoResearch) for Iba-1, or Cy3-conjugated donkey anti-rat IgG (712-165-150, Jackson ImmunoResearch) for NLRP3. Stained tissues were observed using a fluorescence microscopy (Leica DM4000 B LED, LAS V4.12). To quantify the intensity of CD31 and Iba-1, two to four contralateral or ipsilateral images were acquired from each mouse under 40x fluorescence microscopy and the intensity were measured using LAS V4.12 software (Leica).

Cell culture and sENG treatment

BV2 murine microglia (CRL-2468, ATCC, Manassas, VA) and BALB/C mouse primary brain microvascular ECs (BALB-5023, Cell biologics, Chicago ,IL) were cultured with medium containing high glucose (CM002-050, GenDEPOT, Katy TX) 10% fetal bovine serum (F0901-050, GenDEPOT, Katy, TX) and penicillin-streptomycin (CA005, GenDEPOT) at 37 °C in a 5% CO₂ humidified incubator. The medium for BALB/C mouse primary brain microvascular ECs were added ECs growth supplement (E2759, Sigma-Aldrich, St. Louis, MO). The cells were seeded in 6-well plate (5 × 10⁴/well) and treated with recombinant mouse sENG protein (1320-EN-025, R&D systems) for 24 hour. The sENG-treated BV2 conditioned media (sENG-BV2-CM) mixed with ECs medium (50% v/v) and incubated on the ECs.

EC function assays

For scratch-wound assay, the mouse primary brain microvascular ECs were seeded on 24 well plate (2 × 10⁵ cells/ml) in the absence or presence of sENG-BV2-CM and incubated at 37 °C in a 5% CO₂ humidified incubator. After 10 hours, the images were captured under a microscope and analyzed the wound closure rate using ibidi software.

For tube formation, the mouse primary brain microvascular ECs were seeded on Matrigel (356234, Corning, NY) coated at 48 well plate (1 × 10⁵ cells/ml). The ECs were incubated in the medium with or without sENG-BV2-CM at 37 °C in a 5% CO₂ humidified incubator. After 8 hours, the images were captured under a microscope and analyzed the tube formation using ibidi software (Martinsried, Planegg, Germany).

Quantitative Real-Time PCR

Total mRNA was harvested from each BV2 or ECs according to the manufacturer’s protocols (RNeasy mini kit, 74104, Qiagen, Hilden, Germany) and used for cDNA synthesis using a commercial kit (High-Capacity cDNA Reverse Transcription Kits, 4368814, Applied Biosystems, Foster City, CA). The cDNA were used for Real-Time PCR reaction (Applied Biosystems Quant 3 Studio qPCR) using Fast SYBR™ Green Master Mix (Applied Biosystems, 4385612). PCR primers were purchased from Sigma-Aldrich (St. Louis, MO). The following primers were used:

VEGF-A	(F)	CTCACCAAAGCCAGCACATA
	(R)	AATGCTTTCTCCGCTCTGAA
TGFβ	(F)	GCCCTTCCTGCTCCTCATG
	(R)	CCGCACACAGCAGTTCTTCTC
Notch-1	(F)	CTGAGGCAAGGATTGGAGTC
	(R)	GAATGGAGGTAGGTGCGAAG
IL-6	(F)	TGGTACTCCAGAAGACCAGAGG
	(R)	AACGATGATGCACTTGCAGA
TNF-α	(F)	ATGGCCTCCCTCTCATCAGT
	(R)	TTTGCTACGACGTGGGCTAC
MMP-9	(F)	GCCGACTTTTGTGGTCTTCC
	(R)	TACAAGTATGCCTCTGCCAGC

NLRP3 (F) CTTCTAGCTTCTGCCGTGGTCTCT
 (R) CGAAGCAGCATTGATGGGACA
 Caspase-1 (F) GTACACGTCTTGCCCTCATTATCTG
 (R) TTTCACCTCTTTCACCATCTCCAG
 ASC (F) CTGAGCAGCTGCAAACGACTAAA
 (R) CTTCTGTGACCCTGGCAATGAGT
 IL-1 β (F) CAACCAACAAGTGATATTCTCCATG
 (R) GATCCACACTCTCCAGCTGCA
 GAPDH (F) GGAGTCAACGGATTGCTCG
 (R) GGAATCATATTGGAACATGTAAACC

Western blotting

BV2 and ECs were harvested and lysed using a protein lysis buffer (R4100, GenDEPOT, 50 mM Tris-HCl, pH 7.4, 150mM NaCl, 1% triton X-100, 2 mM EDTA, 0.5% Sodium deoxycholate, 0.1% SDS) containing Phosphatase Inhibitor Mixture (P3200-005, GenDEPOT) and Protease Inhibitor Mixture (P3100-005, GenDEPOT). The proteins were separated by electrophoresis in 4-20% ExpressPlus™ Page Gel (M42015, GenScript, Piscataway, NJ) using Mini-PROTEAN Tetra Cell (1658004, Bio-Rad Laboratories, Hercules, CA) and transferred to polyvinylidene difluoride membranes (1704273, Bio-Rad Laboratories) using Trans-Blot Turbo Transfer System (1704150, Bio-Rad Laboratories). The following primary and secondary antibodies were used for the western blot in this study: p-ERK1/2 (Thr202/Tyr204) (1:1,000, 9101, Cell Signaling Technology), t-ERK (1:1,000, 9102, Cell Signaling Technology), IL-17RD (1:1,000, AF2276, R&D systems, Minneapolis, MN,) or β -actin (1:1,000, sc-47778, Santa Cruz Biotechnology). After incubate the blots for 2 hour at 4°C, secondary antibodies used: Rabbit IgG Horseradish Peroxidase-conjugated antibody (1:2,000, HAF008, R&D systems) or Mouse IgG Horseradish Peroxidase-conjugated antibody (1:2,000, HAF007, R&D systems).

Statistical analysis

All values are expressed as mean \pm standard error of the mean. Statistical significance ($P < 0.05$ for all analysis) was assessed by Student's *t*-test or One-way ANOVA using the Instat 3.05 software package (GraphPad Software, San Diego, CA, USA).

Author Contributions: Conceptualization, E.S.P. and E.K.; methodology, E.S.P., S.K.; software, J.P.S.; validation, E.S.P., S.K. and D.C.Y.; formal analysis, E.S.P., S.K., D.C.Y. and E.K.; investigation, E.S.P., E.K.; resources, P.R.C and E.K.; data curation, E.S.P., S.K., D.C.Y., J.P.S., H.A.C, and E.K.; writing—original draft preparation, E.S.P.; writing—review and editing, E.S.P., S.K., D.C.Y., J.P.S., H.A.C., P.R.C. and E.K.; visualization, E.S.P.; supervision, E.S.P. and E.K.; project administration, E.S.P. and E.K.; funding acquisition, P.R.C and E.K. All authors have read and agreed to the published version of the manuscript.

Funding: This work was supported by Weatherhead Foundation and AVM Research Foundation.

Institutional Review Board Statement: The study was conducted according to the guidelines of the Declaration of Helsinki, and approved by the Institutional Review Board (or Ethics Committee) of the University of Texas Health Science Center at Houston (protocol code: AWC-20-0136, updated date of approval: 12-23-2021).

Data Availability Statement: All data generated for this study is available from the corresponding authors upon reasonable request.

Acknowledgments: The authors thank the Dipaolo and Theaker families for generous donations in support of this work.

Conflicts of Interest: The authors declare no conflict of interest.

References

1. Lawton, M.T., W.C. Rutledge, H. Kim, C. Stapf, K.J. Whitehead, D.Y. Li, T. Krings, K. terBrugge, D. Kondziolka, M.K. Morgan, K. Moon, and R.F. Spetzler, Brain arteriovenous malformations. *Nat Rev Dis Primers* **2015**, *1*, 15008.
2. Solomon, R.A. and E.S. Connolly, Jr., Arteriovenous Malformations of the Brain. *N Engl J Med* **2017**, *376*, 1859-1866.
3. Bayrak-Toydemir, P., J. McDonald, B. Markewitz, S. Lewin, F. Miller, L.S. Chou, F. Gedge, W. Tang, H. Coon, and R. Mao, Genotype-phenotype correlation in hereditary hemorrhagic telangiectasia: mutations and manifestations. *Am J Med Genet A* **2006**, *140*, 463-470.
4. Govani, F.S. and C.L. Shovlin, Hereditary haemorrhagic telangiectasia: a clinical and scientific review. *Eur J Hum Genet* **2009**, *17*, 860-871.
5. Sabba, C., G. Pasculli, G.M. Lenato, P. Suppressa, P. Lastella, M. Memeo, F. Dicunzo, and G. Guant, Hereditary hemorrhagic telangiectasia: clinical features in ENG and ALK1 mutation carriers. *J Thromb Haemost* **2007**, *5*, 1149-1157.
6. Rossi, E., C. Bernabeu, and D.M. Smadja, Endoglin as an Adhesion Molecule in Mature and Progenitor Endothelial Cells: A Function Beyond TGF-beta. *Front Med (Lausanne)* **2019**, *6*, 10.
7. Albinana, V., M.P. Zafra, J. Colau, R. Zarrabeitia, L. Recio-Poveda, L. Olavarrieta, J. Perez-Perez, and L.M. Botella, Mutation affecting the proximal promoter of Endoglin as the origin of hereditary hemorrhagic telangiectasia type 1. *BMC Med Genet* **2017**, *18*, 20.
8. Choi, E.J., W. Chen, K. Jun, H.M. Arthur, W.L. Young, and H. Su, Novel brain arteriovenous malformation mouse models for type 1 hereditary hemorrhagic telangiectasia. *PLoS One* **2014**, *9*, e88511.
9. Chen, Y., Q. Hao, H. Kim, H. Su, M. Letarte, S.A. Karumanchi, M.T. Lawton, N.M. Barbaro, G.Y. Yang, and W.L. Young, Soluble endoglin modulates aberrant cerebral vascular remodeling. *Ann Neurol* **2009**, *66*, 19-27.
10. Mouchtouris, N., P.M. Jabbour, R.M. Starke, D.M. Hasan, M. Zanaty, T. Theofanis, D. Ding, S.I. Tjoumakaris, A.S. Dumont, G.M. Ghobrial, D. Kung, R.H. Rosenwasser, and N. Chalouhi, Biology of cerebral arteriovenous malformations with a focus on inflammation. *J Cereb Blood Flow Metab* **2015**, *35*, 167-175.
11. Zhang, R., Z. Han, V. Degos, F. Shen, E.J. Choi, Z. Sun, S. Kang, M. Wong, W. Zhu, L. Zhan, H.M. Arthur, S.P. Oh, M.E. Faughnan, and H. Su, Persistent infiltration and pro-inflammatory differentiation of monocytes cause unresolved inflammation in brain arteriovenous malformation. *Angiogenesis* **2016**, *19*, 451-461.
12. Chen, Y., W. Zhu, A.W. Bollen, M.T. Lawton, N.M. Barbaro, C.F. Dowd, T. Hashimoto, G.Y. Yang, and W.L. Young, Evidence of inflammatory cell involvement in brain arteriovenous malformations. *Neurosurgery* **2008**, *62*, 1340-1349; discussion 1349-1350.
13. Germans, M.R., W. Sun, M. Sebok, A. Keller, and L. Regli, Molecular Signature of Brain Arteriovenous Malformation Hemorrhage: A Systematic Review. *World Neurosurg* **2022**, *157*, 143-151.
14. Varejckova, M., E. Gallardo-Vara, M. Vicen, B. Vitverova, P. Fikrova, E. Dolezelova, J. Rathouska, A. Prasnicka, K. Blazickova, S. Micuda, C. Bernabeu, I. Nemeckova, and P. Nachtigal, Soluble endoglin modulates the pro-inflammatory mediators NF-kappaB and IL-6 in cultured human endothelial cells. *Life Sci* **2017**, *175*, 52-60.
15. Guo, Y., T. Tihan, H. Kim, C. Hess, M.T. Lawton, W.L. Young, Y. Zhao, and H. Su, Distinctive distribution of lymphocytes in unruptured and previously untreated brain arteriovenous malformation. *Neuroimmunol Neuroinflamm* **2014**, *1*, 147-152.
16. Park, E.S., S. Kim, S. Huang, J.Y. Yoo, J. Korbelin, T.J. Lee, B. Kaur, P.K. Dash, P.R. Chen, and E. Kim, Selective Endothelial Hyperactivation of Oncogenic KRAS Induces Brain Arteriovenous Malformations in Mice. *Ann Neurol* **2021**, *89*, 926-941.
17. Eggen, B.J., D. Raj, U.K. Hanisch, and H.W. Boddeke, Microglial phenotype and adaptation. *J Neuroimmune Pharmacol* **2013**, *8*, 807-823.
18. Kettenmann, H., U.K. Hanisch, M. Noda, and A. Verkhratsky, Physiology of microglia. *Physiol Rev* **2011**, *91*, 461-553.
19. Kreutzberg, G.W., Microglia: a sensor for pathological events in the CNS. *Trends Neurosci* **1996**, *19*, 312-318.

20. Shirasuna, K., T. Karasawa, and M. Takahashi, Role of the NLRP3 Inflammasome in Preeclampsia. *Front Endocrinol (Lausanne)* **2020**, *11*, 80.
21. Jabbour, M.N., J.B. Elder, C.G. Samuelson, S. Khashabi, F.M. Hofman, S.L. Giannotta, and C.Y. Liu, Aberrant angiogenic characteristics of human brain arteriovenous malformation endothelial cells. *Neurosurgery* **2009**, *64*, 139-146; discussion 146-138.
22. Ding, X., R. Gu, M. Zhang, H. Ren, Q. Shu, G. Xu, and H. Wu, Microglia enhanced the angiogenesis, migration and proliferation of co-cultured RMECs. *BMC Ophthalmol* **2018**, *18*, 249.
23. Nikolaev, S.I., S. Vetiska, X. Bonilla, E. Boudreau, S. Jauhiainen, B. Rezai Jahromi, N. Khyzha, P.V. DiStefano, S. Suutarinen, T.R. Kiehl, V. Mendes Pereira, A.M. Herman, T. Krings, H. Andrade-Barazarte, T. Tung, T. Valiante, G. Zadeh, M. Tymianski, T. Rauramaa, S. Yla-Herttuala, J.D. Wythe, S.E. Antonarakis, J. Frosen, J.E. Fish, and I. Radovanovic, Somatic Activating KRAS Mutations in Arteriovenous Malformations of the Brain. *N Engl J Med* **2018**, *378*, 250-261.
24. Cai, J., E. Pardali, G. Sanchez-Duffhues, and P. ten Dijke, BMP signaling in vascular diseases. *FEBS Lett* **2012**, *586*, 1993-2002.
25. Pardali, E., M.J. Goumans, and P. ten Dijke, Signaling by members of the TGF-beta family in vascular morphogenesis and disease. *Trends Cell Biol* **2010**, *20*, 556-567.
26. Pardali, E. and P. Ten Dijke, TGFbeta signaling and cardiovascular diseases. *Int J Biol Sci* **2012**, *8*, 195-213.
27. Yao, Y., J. Yao, M. Radparvar, A.M. Blazquez-Medela, P.J. Guihard, M. Jumabay, and K.I. Bostrom, Reducing Jagged 1 and 2 levels prevents cerebral arteriovenous malformations in matrix Gla protein deficiency. *Proc Natl Acad Sci U S A* **2013**, *110*, 19071-19076.
28. Barbosa Do Prado, L., C. Han, S.P. Oh, and H. Su, Recent Advances in Basic Research for Brain Arteriovenous Malformation. *Int J Mol Sci* **2019**, *20*,
29. ZhuGe, Q., M. Zhong, W. Zheng, G.Y. Yang, X. Mao, L. Xie, G. Chen, Y. Chen, M.T. Lawton, W.L. Young, D.A. Greenberg, and K. Jin, Notch-1 signalling is activated in brain arteriovenous malformations in humans. *Brain* **2009**, *132*, 3231-3241.
30. Darby, S., K. Sahadevan, M.M. Khan, C.N. Robson, H.Y. Leung, and V.J. Gnanapragasam, Loss of Sef (similar expression to FGF) expression is associated with high grade and metastatic prostate cancer. *Oncogene* **2006**, *25*, 4122-4127.
31. Girondel, C., K. Levesque, M.J. Langlois, S. Pasquin, M.K. Saba-El-Leil, N. Rivard, R. Friesel, M.J. Servant, J.F. Gauchat, S. Lesage, and S. Meloche, Loss of interleukin-17 receptor D promotes chronic inflammation-associated tumorigenesis. *Oncogene* **2021**, *40*, 452-464.
32. Ku, Y.H., B.J. Cho, M.J. Kim, S. Lim, Y.J. Park, H.C. Jang, and S.H. Choi, Rosiglitazone increases endothelial cell migration and vascular permeability through Akt phosphorylation. *BMC Pharmacol Toxicol* **2017**, *18*, 62.
33. Lamalice, L., F. Le Boeuf, and J. Huot, Endothelial cell migration during angiogenesis. *Circ Res* **2007**, *100*, 782-794.
34. Lusis, A.J., Atherosclerosis. *Nature* **2000**, *407*, 233-241.
35. Goumans, M.J., F. Lebrin, and G. Valdimarsdottir, Controlling the angiogenic switch: a balance between two distinct TGF-beta receptor signaling pathways. *Trends Cardiovasc Med* **2003**, *13*, 301-307.
36. ten Dijke, P. and H.M. Arthur, Extracellular control of TGFbeta signalling in vascular development and disease. *Nat Rev Mol Cell Biol* **2007**, *8*, 857-869.
37. McAllister, K.A., K.M. Grogg, D.W. Johnson, C.J. Gallione, M.A. Baldwin, C.E. Jackson, E.A. Helmbold, D.S. Markel, W.C. McKinnon, J. Murrell, and et al., Endoglin, a TGF-beta binding protein of endothelial cells, is the gene for hereditary haemorrhagic telangiectasia type 1. *Nat Genet* **1994**, *8*, 345-351.
38. Satomi, J., R.J. Mount, M. Toporsian, A.D. Paterson, M.C. Wallace, R.V. Harrison, and M. Letarte, Cerebral vascular abnormalities in a murine model of hereditary hemorrhagic telangiectasia. *Stroke* **2003**, *34*, 783-789.
39. Kumar, S., C.C. Pan, J.C. Bloodworth, A.B. Nixon, C. Theuer, D.G. Hoyt, and N.Y. Lee, Antibody-directed coupling of endoglin and MMP-14 is a key mechanism for endoglin shedding and deregulation of TGF-beta signaling. *Oncogene* **2014**, *33*, 3970-3979.

40. Hashimoto, T., G. Wen, M.T. Lawton, N.J. Boudreau, A.W. Bollen, G.Y. Yang, N.M. Barbaro, R.T. Higashida, C.F. Dowd, V.V. Halbach, W.L. Young, and S.F.B.S.G. University of California, Abnormal expression of matrix metalloproteinases and tissue inhibitors of metalloproteinases in brain arteriovenous malformations. *Stroke* **2003**, *34*, 925-931.
41. Hawinkels, L.J., P. Kuiper, E. Wiercinska, H.W. Verspaget, Z. Liu, E. Pardali, C.F. Sier, and P. ten Dijke, Matrix metalloproteinase-14 (MT1-MMP)-mediated endoglin shedding inhibits tumor angiogenesis. *Cancer Res* **2010**, *70*, 4141-4150.
42. Rathouska, J., K. Jezkova, I. Nemeckova, and P. Nachtigal, Soluble endoglin, hypercholesterolemia and endothelial dysfunction. *Atherosclerosis* **2015**, *243*, 383-388.
43. Venkatesha, S., M. Toporsian, C. Lam, J. Hanai, T. Mammoto, Y.M. Kim, Y. Bdolah, K.H. Lim, H.T. Yuan, T.A. Libermann, I.E. Stillman, D. Roberts, P.A. D'Amore, F.H. Epstein, F.W. Sellke, R. Romero, V.P. Sukhatme, M. Letarte, and S.A. Karumanchi, Soluble endoglin contributes to the pathogenesis of preeclampsia. *Nat Med* **2006**, *12*, 642-649.
44. Lawera, A., Z. Tong, M. Thorikay, R.E. Redgrave, J. Cai, M. van Dinther, N.W. Morrell, G.B. Afink, D.S. Charnock-Jones, H.M. Arthur, P. Ten Dijke, and W. Li, Role of soluble endoglin in BMP9 signaling. *Proc Natl Acad Sci U S A* **2019**, *116*, 17800-17808.
45. Lopez-Novoa, J.M. and C. Bernabeu, The physiological role of endoglin in the cardiovascular system. *Am J Physiol Heart Circ Physiol* **2010**, *299*, H959-974.
46. Cheng, P., L. Ma, S. Shaligram, E.J. Walker, S.T. Yang, C. Tang, W. Zhu, L. Zhan, Q. Li, X. Zhu, M.T. Lawton, and H. Su, Effect of elevation of vascular endothelial growth factor level on exacerbation of hemorrhage in mouse brain arteriovenous malformation. *J Neurosurg* **2019**, *132*, 1566-1573.
47. Juraskova, B., C. Andrys, I. Holmerova, D. Solichova, D. Hrnčiarikova, H. Vankova, T. Vasatko, and J. Krejsek, Transforming growth factor beta and soluble endoglin in the healthy senior and in Alzheimer's disease patients. *J Nutr Health Aging* **2010**, *14*, 758-761.
48. Saita, E., K. Miura, N. Suzuki-Sugihara, K. Miyata, N. Ikemura, R. Ohmori, Y. Ikegami, Y. Kishimoto, K. Kondo, and Y. Momiyama, Plasma Soluble Endoglin Levels Are Inversely Associated With the Severity of Coronary Atherosclerosis-Brief Report. *Arterioscler Thromb Vasc Biol* **2017**, *37*, 49-52.
49. Blazquez-Medela, A.M., L. Garcia-Ortiz, M.A. Gomez-Marcos, J.I. Recio-Rodriguez, A. Sanchez-Rodriguez, J.M. Lopez-Novoa, and C. Martinez-Salgado, Increased plasma soluble endoglin levels as an indicator of cardiovascular alterations in hypertensive and diabetic patients. *BMC Med* **2010**, *8*, 86.
50. Gallardo-Vara, E., S. Tual-Chalot, L.M. Botella, H.M. Arthur, and C. Bernabeu, Soluble endoglin regulates expression of angiogenesis-related proteins and induction of arteriovenous malformations in a mouse model of hereditary hemorrhagic telangiectasia. *Dis Model Mech* **2018**, *11*,
51. Dudiki, T., J. Meller, G. Mahajan, H. Liu, I. Zhevlakova, S. Stefl, C. Witherow, E. Podrez, C.R. Kothapalli, and T.V. Byzova, Microglia control vascular architecture via a TGFbeta1 dependent paracrine mechanism linked to tissue mechanics. *Nat Commun* **2020**, *11*, 986.
52. Cheadle, L., S.A. Rivera, J.S. Phelps, K.A. Ennis, B. Stevens, L.C. Burkly, W.A. Lee, and M.E. Greenberg, Sensory Experience Engages Microglia to Shape Neural Connectivity through a Non-Phagocytic Mechanism. *Neuron* **2020**, *108*, 451-468 e459.
53. Hagemeyer, N., K.M. Hanft, M.A. Akritidou, N. Unger, E.S. Park, E.R. Stanley, O. Staszewski, L. Dimou, and M. Prinz, Microglia contribute to normal myelinogenesis and to oligodendrocyte progenitor maintenance during adulthood. *Acta Neuropathol* **2017**, *134*, 441-458.
54. Chitu, V., F. Biundo, G.G.L. Shlager, E.S. Park, P. Wang, M.E. Gulinello, S. Gokhan, H.C. Ketchum, K. Saha, M.A. DeTure, D.W. Dickson, Z.K. Wszolek, D. Zheng, A.L. Croxford, B. Becher, D. Sun, M.F. Mehler, and E.R. Stanley, Microglial Homeostasis Requires Balanced CSF-1/CSF-2 Receptor Signaling. *Cell Rep* **2020**, *30*, 3004-3019 e3005.
55. Diaz-Aparicio, I., I. Paris, V. Sierra-Torre, A. Plaza-Zabala, N. Rodriguez-Iglesias, M. Marquez-Ropero, S. Beccari, P. Huguet, O. Abiega, E. Alberdi, C. Matute, I. Bernales, A. Schulz, L. Otrokoci, B. Sperlagh, K.E. Happonen, G. Lemke, M. Maletic-

- Savatic, J. Valero, and A. Sierra, Microglia Actively Remodel Adult Hippocampal Neurogenesis through the Phagocytosis Secretome. *J Neurosci* **2020**, *40*, 1453-1482.
56. Sierra-Torre, V., A. Plaza-Zabala, P. Bonifazi, O. Abiega, I. Diaz-Aparicio, S. Tegelberg, A.E. Lehesjoki, J. Valero, and A. Sierra, Microglial phagocytosis dysfunction in the dentate gyrus is related to local neuronal activity in a genetic model of epilepsy. *Epilepsia* **2020**, *61*, 2593-2608.
 57. Willis, E.F., K.P.A. MacDonald, Q.H. Nguyen, A.L. Garrido, E.R. Gillespie, S.B.R. Harley, P.F. Bartlett, W.A. Schroder, A.G. Yates, D.C. Anthony, S. Rose-John, M.J. Ruitenberg, and J. Vukovic, Repopulating Microglia Promote Brain Repair in an IL-6-Dependent Manner. *Cell* **2020**, *180*, 833-846 e816.
 58. Bisht, K., K.A. Okojie, K. Sharma, D.H. Lentferink, Y.Y. Sun, H.R. Chen, J.O. Uweru, S. Amancherla, Z. Calcuttawala, A.B. Campos-Salazar, B. Corliss, L. Jabbour, J. Benderoth, B. Friestad, W.A. Mills, 3rd, B.E. Isakson, M.E. Tremblay, C.Y. Kuan, and U.B. Eyo, Capillary-associated microglia regulate vascular structure and function through PANX1-P2RY12 coupling in mice. *Nat Commun* **2021**, *12*, 5289.
 59. Iadecola, C., The Neurovascular Unit Coming of Age: A Journey through Neurovascular Coupling in Health and Disease. *Neuron* **2017**, *96*, 17-42.
 60. Kisler, K., A.M. Nikolakopoulou, and B.V. Zlokovic, Microglia have a grip on brain microvasculature. *Nat Commun* **2021**, *12*, 5290.
 61. Walker, D.G., L.F. Lue, T.G. Beach, and I. Tooyama, Microglial Phenotyping in Neurodegenerative Disease Brains: Identification of Reactive Microglia with an Antibody to Variant of CD105/Endoglin. *Cells* **2019**, *8*,
 62. Gougos, A. and M. Letarte, Primary structure of endoglin, an RGD-containing glycoprotein of human endothelial cells. *J Biol Chem* **1990**, *265*, 8361-8364.
 63. Lastres, P., T. Bellon, C. Cabanas, F. Sanchez-Madrid, A. Acevedo, A. Gougos, M. Letarte, and C. Bernabeu, Regulated expression on human macrophages of endoglin, an Arg-Gly-Asp-containing surface antigen. *Eur J Immunol* **1992**, *22*, 393-397.
 64. O'Connell, P.J., A. McKenzie, N. Fisicaro, S.P. Rockman, M.J. Pearse, and A.J. d'Apice, Endoglin: a 180-kD endothelial cell and macrophage restricted differentiation molecule. *Clin Exp Immunol* **1992**, *90*, 154-159.
 65. Timis, T.L., I.A. Florian, S. Susman, and I.S. Florian, Involvement of Microglia in the Pathophysiology of Intracranial Aneurysms and Vascular Malformations-A Short Overview. *Int J Mol Sci* **2021**, *22*,
 66. Al-Shahi, R., J.S. Fang, S.C. Lewis, and C.P. Warlow, Prevalence of adults with brain arteriovenous malformations: a community based study in Scotland using capture-recapture analysis. *J Neurol Neurosurg Psychiatry* **2002**, *73*, 547-551.
 67. Kandai, S., M.S. Abdullah, and N.N. Naing, Angioarchitecture of brain arteriovenous malformations and the risk of bleeding: an analysis of patients in northeastern malaysia. *Malays J Med Sci* **2010**, *17*, 44-48.